Laser ultrasonics for in-situ monitoring of microstructure evolution in steels

MILITZER Matthias[1], GARCIN Thomas[1], KULAKOV Mykola[1] and POOLE Warren[1]
[1]The Centre for Metallurgical Process Engineering,
The University of British Columbia,
309-6350 Stores Rd., Vancouver, BC, Canada V6T 1Z4

Abstract: Laser ultrasonics for metallurgy (LUMet) is an innovative sensor technology for in-situ measurement of microstructure evolution during thermomechanical processing. Laser ultrasonics is a technique which is fast, remote and particularly adapted to measurements at high temperatures during complex thermomechanical processing paths. Recent advances in this technique will be illustrated with laboratory studies using a Gleeble 3500 thermomechanical simulator with a LUMet attachment. The LUMet technique has been used to measure austenite grain growth, austenite formation and decomposition in low-carbon steels during heating-cooling cycles, as well as ferrite recrystallization during annealing of cold-rolled steels. The LUMet measurements have been validated with conventional metallographic data. In particular, these studies have been focused on thermal cycles for the heat affected zone in an API-X80 linepipe steel as well as for intercritical annealing treatments of a DP600 steel that are typical for hot dip galvanizing lines. These examples are used to show the significance of this new sensor technology to accelerate the development of metallurgical process models for advanced steels. Even though a number of limitations exists, the LUMet system offers exciting opportunities for process development in the laboratory and process control in the plant.

Key words: Steel; Laser ultrasonics; Austenite grain growth; Phase transformation; Recrystallization

1 Introduction

Advanced High Strength Steel (AHSS) are an important material class to enable sustainable solutions in transportation, infrastructure and energy. For example, in the pipeline industry, the development of high strength linepipe steels is critical for the construction of gas and oil transmission lines with larger diameter and operating at higher pressure [1,2,3]. State-of-the-art linepipe steels are low carbon steels that are microalloyed with Nb, Ti and other elements (e.g. V, Mo) as required to combine excellent weldability with high strength and fracture toughness. A particular concern for the integrity of pipelines is the heat affected zone (HAZ) of girth welds, i.e. when pipe sections are welded in the field. There is a need to implement new, more efficient welding procedures, e.g. dual-torch and laser-hybrid welding. The rapid thermal cycles during welding lead to microstructure gradients in the HAZ that may critically affect their mechanical properties [4]. In particular the formation of microstructures with reduced resistance to crack propagation is of concern. Therefore, there is significant interest to develop microstructure modelling tools that can predict the microstructure evolution as a function of the welding process parameters [5]. Another important example for the use of AHSS is found in the automotive industry where Dual Phase (DP) steels have become a material of choice as they offer a superior combination of strength, drawability and crashworthiness [6]. Embedding hard microstructure constituents (i.e. martensitic or bainite) into a soft ferritic matrix leads to automotive sheets with high strain hardening. The formation of these complex microstructures requires control of the rolling and annealing steps and a correct comprehension of the metallurgical processes leading to the final properties of the steel. Here again, microstructure modelling tools are crucial to develop and optimize

processing strategies to meet property targets consistently and with low variability.

These metallurgical models for microstructure prediction are conventionally developed by laboratory testing that includes labour intensive post mortem characterization of microstructures. Therefore, tools to monitor the evolution of the microstructure during the high temperature processing of specimens can significantly accelerate the model development and, thus, expedite the implementation of new and/or improved processing routes. Laser ultrasonics for metallurgy (LUMet) is an emerging technology dedicated to the in-situ monitoring of microstructure parameters during materials processing [7]. In this technique, lasers are used for the generation and detection of ultrasound pulse in the material. The characteristics of the ultrasound waves are functions of the microstructure. Ultrasonic velocity is related to the elastic constants and the density, i.e. it depends on the crystal structure and texture, whereas ultrasonic attenuation is primarily related to grain size, dislocation density and porosity. Methods were developed to correlate laser ultrasonic measurements in steel with the austenite grain size [8,9,10], the recrystallization of ferrite [11,12] and austenite [13,14], as well as the austenite decomposition during cooling [15,16]. These studies examined the potential of laser ultrasonics during thermal treatments specifically designed for studies in the laboratory. As a result, the LUMet system was designed as an attachment to a Gleeble thermo-mechanical simulator such that the technique can now be used more routinely to monitor microstructure evolution during laboratory simulated industrial processing cycles.

In this paper, capabilities of LUMet are illustrated with measurements on state-of-the-art steels for two processes with significant industrial relevance. First, the application of laser ultrasonics is described to measure formation, grain growth and decomposition of austenite in an API-X80 linepipe steel during simulated weld thermal cycles. Then, a cold-rolled DP600 steel is examined with LUMet during simulated intercritical annealing treatments. Laser ultrasonic measurements are validated with conventional metallographic observations and dilation data.

2 Experimental

2.1 LUMet sensor and ultrasound parameters

The laboratory simulations were carried out in a Gleeble 3500 thermomechanical simulator coupled with the newly developed LUMet system as an attachment to the rear door of the Gleeble machine. The laser ultrasonic measurements are conducted inside the Gleeble chamber in the centre of the sample in the pulse-echo configuration. A frequency-doubled Q-switched Nd:YAG laser with a wavelength of 532 nm is used for the generation of a wide band compressive ultrasound pulse. The duration of the laser pulse is approximately 6 ns and has a maximum energy of 72 mJ. The laser pulse produces a longitudinal ultrasound pulse by vaporizing a small quantity of material at the surface (of the order of a micron per hundred laser pulses). The ultrasound pulse propagates back and forth through the thickness of the sample and its amplitude decreases by interacting with the material and its microstructure. Successive arrival of the ultrasound pulse at the generation surface is detected with a frequency-stabilized Nd:YAG laser which illuminates the surface with an infrared radiation at a wave length of 1064 μm and pulse duration of 90 μs. The infrared detection laser light reflected on the specimen surface is demodulated inside a photo-refractive crystal using an active interferometer approach [17]. The ultrasound properties measured in this technique are representative of the average properties of the material over a volume created by the surface of the laser spot with a typical diameter of 2 mm multiplied by the sample thickness (typically

1-2 mm). An improvement of the statistics is obtained for larger thickness which is particularly important when measuring coarser microstructures.

The ultrasonic longitudinal velocity is experimentally obtained from the ultrasound signal by the ratio of the propagation distance to the delay between two successive echoes. The compressive wave velocity is a function of the elastic modulus of the material in the propagation direction. The cold-rolled material exhibits a deformation texture that results in a macroscopic anisotropy of velocity in the through thickness direction of the sample. During recrystallization, a new family of grains forms from the deformed structure resulting in a modification of the bulk texture in the material. These texture variations are directly associated with the variation of the ultrasonic wave velocity. Variation of velocity can also be used to investigate the occurrence of phase transformation such as austenite formation and decomposition as long as the difference between the elastic properties of the parent and product phase is sufficiently large. Ultrasonic grain size measurements are based on monitoring attenuation. In highly anisotropic materials like steel, the ultrasonic attenuation resulting from scattering by grains is extracted from other dispersive contributions using a signal from a fine grained reference sample where contributions from grain scattering are negligible. The part of the attenuation due to grain scattering is then expressed as a function of average grain size and frequency. A suitable calibration was provided by Kruger et al. for austenite grain size in a range of plain C-Mn steels [9].

2.2 Materials and procedure

Two state-of-the-art commercial steels were investigated in this study. A hot-rolled API-X80 linepipe steel with a chemistry (key elements in wt. pct.) of 0.06C-1.65Mn-0.24Mo-0.034Nb-0.012Ti-0.005N was supplied by Evraz Inc. NA (Regina, SK). The as-received microstructure consists of irregular ferrite, including randomly distributed martensite/austenite (M/A) islands and complex precipitates. The precipitates ranging between 3 and 100 nm, can be grouped into four classes: TiN, small and large NbCN and Mo_2C [4]. A DP600 steel with a chemistry (key elements in wt. pct.) of 0.10C-1.86Mn-0.16Si-0.34Cr was supplied by ArcelorMittal Dofasco (Hamilton, ON) in form of 50% cold-rolled sheets with a thickness of 1.8 mm. The microstructure of these sheets consists of a ferrite-bainite matrix with elongated grains and 5% pearlite. For laser ultrasound analysis, samples were machined from the as-received materials as rectangular sheet specimen of 10 mm in width, 60 mm in length and 1.5 mm in thickness for the API-X80 steel and 1.8 mm thickness for the DP600 steel.

Laser ultrasonic measurements were conducted for both steels using first simplified heat treatments before extending studies to simulated heating cycles of direct industrial relevance. The study on the API-X80 linepipe steel emphasized heat treatment conditions that typically occur in the HAZ of girth welds. First, simplified heating and cooling paths were studied. Subsequently, a heat treatment cycle was investigated that was concluded from a dual torch welding trial (see Fig. 1a). Here, the time-temperature path is based on the solution of the Rosenthal equation for thick plate as described elsewhere [18]. The rapid heating steps were conducted at a rate of 100 ºC/s to peak temperatures of 1240 and 1210 ºC for the first and second pass, respectively. As the cooling rates are not constant in this scenario, they are characterized by the time required for the temperature to drop from 800 to 500 ºC, i.e. 7 and 20 s for the first and second pass, which corresponds to average cooling rates of 40 and 15 ºC/s, respectively.

The study on the DP steel was emphasizing intercritical annealing simulations of 50% cold-rolled sheet specimens. First, isothermal and continuous heating tests were investigated. Then,

the cold-rolled samples were heat treated to simulate an intercritical annealing cycle as illustrated in Fig. 1b. Here, the cold-rolled sample was heated at 1 ºC/s to 770 ºC where the sample was held for 10 min. The samples were then cooled at a constant rate of 3 ºC/s and held at 465 ºC for 3 min prior to rapid cooling to room temperature. The holding at 465 ºC simulates the coating process in the zinc bath of a hot dip galvanizing line.

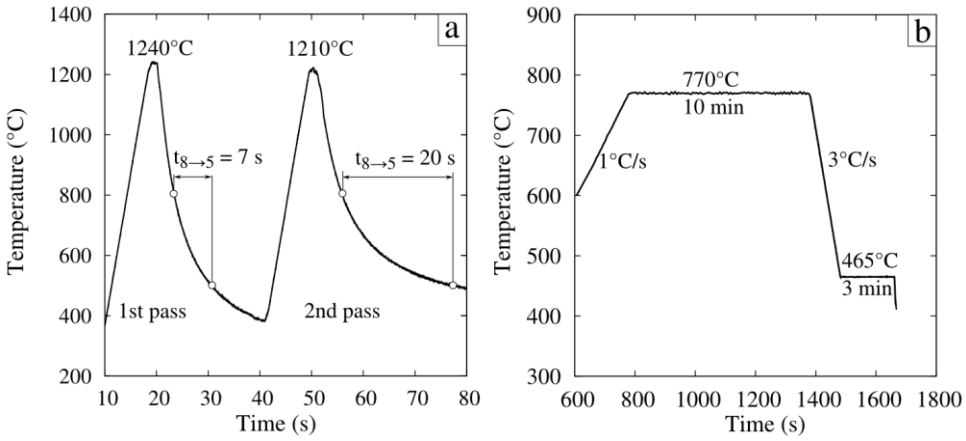

Fig. 1 a) Heat treatment cycle applied to the API-X80 linepipe steel to simulate dual-torch welding, b) Intercritical annealing cycle applied to the DP600 steel

The temperature of the sample was controlled using a thermocouple spot welded at the centre of the samples; S-type thermocouples were employed for the API-X80 steel and K-type thermocouples for the DP600 steel. The dilation of the specimen width was measured simultaneously with the laser ultrasonic inspection. For this purpose a LVDT dilatometer was installed in the same isothermal line than that of the thermocouple and laser spots. Further, conventional metallographic studies were conducted to determine fraction recrystallized and grain size at selected positions of the heat treatment cycles. The austenite grain size is expressed in terms of the equivalent area grain diameter. The metallographic and dilation data were used to benchmark the laser ultrasonic measurements.

3. Results and discussion

3.1 API-X80 steel

3.1.1 Continuous heating and cooling thermal cycles

The evolution of the ultrasound attenuation measured at a frequency of 10 MHz and the ultrasound velocity is shown in Fig. 2a as a function of temperature during the rapid continuous heating at 100 °C/s of the as-received API-X80 steel. The temperature dependence of the ultrasound velocity shows three stages, that can be summarized as follow: (i) a non-linear decrease with increasing temperature up to 730 °C, (ii) a second decrease at a rate of about 0.9 m/s/°C from 730 to 830 °C where a sudden raise of the velocity by 11 m/s is monitored and, (iii) a linear decrease at a rate of 0.5 m/s/°C above 900 °C. The ultrasound attenuation at 10 MHz decreases almost linearly with increasing temperature from 400 to 680 °C. At this temperature, the attenuation starts to increase and reaches a maximum at 780 °C (about 1 dB/mm higher than at 680 °C). The attenuation then decreases by about 0.5 dB/mm until 860 °C is reached. At higher temperatures, the attenuation increases linearly with temperature.

The dilatometer measurements provide direct information on austenite formation. For

comparison, start (5%) and finish (95%) of this phase transformation are indicated by the symbols in Fig. 2a. Clearly, the decrease in attenuation between 780 and 860 °C correlates well with the austenite formation temperature range whereas no specific variation of the velocity is measured in the beginning of the austenite formation indicating that the velocity of ferrite and austenite are very close in this temperature range. The origin of the velocity increase before the end of the transformation has yet to be further investigated but may be associated with a texture variation in the final transformation stages. In the ferrite region at lower temperatures the laser ultrasonic measurements are primarily affected by magnetism. The non-linear velocity behaviour is associated with the non-linear temperature dependence of the magnetic component in the elastic constants for the ferrite phase [19]. The onset of the second stage, i.e. linear velocity temperature dependence, corresponds to the Curie temperature of the ferrite phase [16]. Interestingly, attenuation sharply increases in the range around the Curie temperature suggesting a significant change in magnetic damping [21]. On the other hand, the linear portions in attenuation and velocity for higher temperatures are characteristics of single phase austenite. In terms of velocity, this linear dependence reflects the linear temperature dependence of the elastic constants whereas the apparent linear increase of attenuation can be correlated with austenite grain growth. The method shown in [9] is then used to correlate the size of austenite grains to the frequency dependence of the attenuation spectrum. As illustrated in Fig. 2b, there is an excellent agreement between the grain sizes measured by laser ultrasonics and metallography. The austenite grain size increases from 5 μm at 950 °C to 35 μm at 1350 °C. Laser ultrasonic measurements could only be extended to 1300 °C because the signal to noise ratio becomes too large to make meaningful measurements at even higher temperatures.

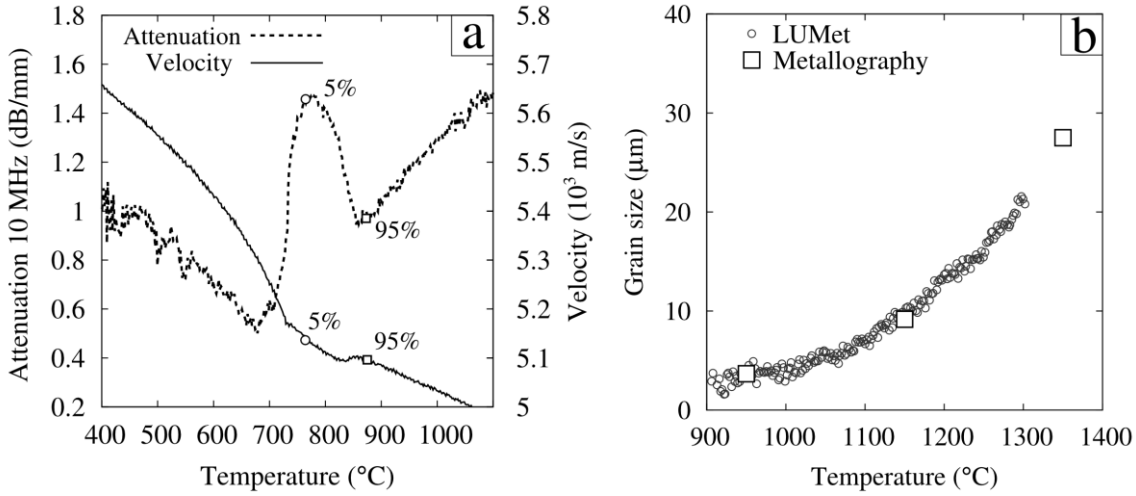

Fig. 2 Laser ultrasonic and conventional measurements of microstructure evolution during heating of the API-X80 steel at a rate of 100 ºC/s: a) Evolution of the ultrasound velocity and attenuation, temperatures for start (5%, circles) and finish (95%, squares) of austenite formation as determined with dilatometry; b) Comparison of laser ultrasonic and metallographic measurements of austenite grain growth

Fig. 3a shows the variation of the ultrasonic velocity during heating and cooling in the austenite decomposition temperature region; the sample was cooled after holding for 7 s at 1300 °C. A lever-rule method can be applied on the velocity signal in order to determine the austenite fraction transformed. The lever rule is employed between the velocity of ferrite measured upon heating and the linear extrapolation of the temperature dependence of the velocity in austenite as illustrated in Fig. 3a. The comparison between the fractions

transformed measured by conventional dilatometry and through the lever rule analysis of the velocity changes is shown in Fig. 3b. The excellent agreement found between the two methods shows that the measurement of velocity during rapid cooling can be used to determine the austenite decomposition kinetics that occurs here in the range between 500 and 400 °C where ultrasound velocities in ferrite and austenite are significantly different because of the ferromagnetic state of ferrite. Referring to the above discussed austenite formation suggests that ultrasound velocity can be used to measure austenite-ferrite transformations provided they occur below the Curie temperature.

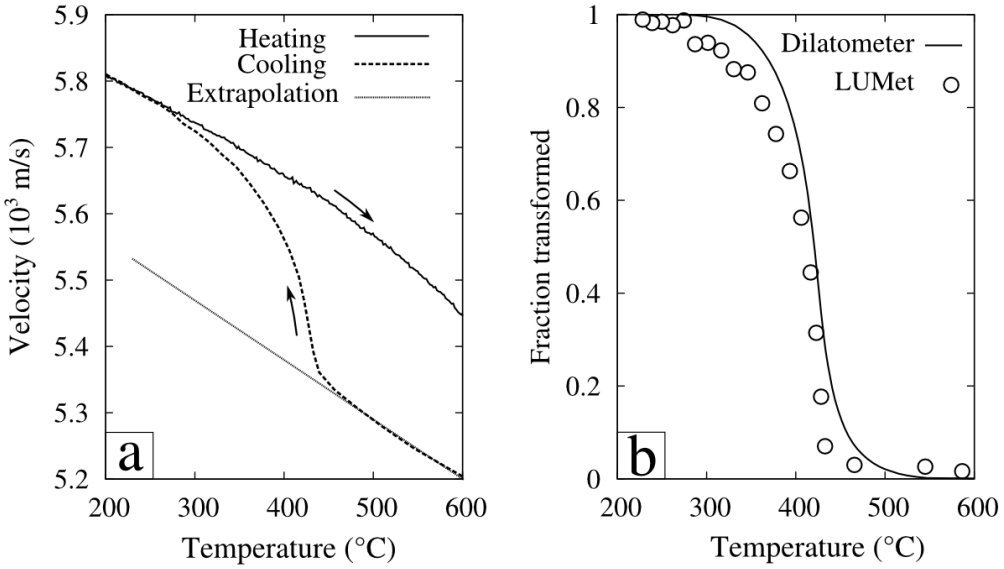

Fig. 3 a) Ultrasonic velocity during heating at 100 ºC/s and continuous cooling at 150 ºC/s in the API-X80 steel; b) comparison of austenite decomposition kinetics as measured by dilatometry and ultrasonic velocity.

3.1.2 Simulation of dual-torch welding

Austenite grain growth measured by LUMet during the two simulated welding passes is shown in Fig. 4a as a function of temperature. During the first pass, the austenite grain growth rate gradually increases upon reaching the peak temperature. However, the measured growth rate is constant during the second pass. According to a previous investigation of the stability of precipitates in austenite for this steel, NbCN precipitates are expected to be almost completely dissolved after reaching the peak temperature during the first pass [4,10]. The increased growth rate at lower temperature in the second cycle is therefore consistent with a reduction of the grain boundary pinning due to the dissolution of these precipitates. The final grain size of approximately 30 μm is, however, similar for both passes as the second peak temperature is 30 °C lower (see Fig. 1a).

The measurements of velocity and dilation during the cooling stages are used to evaluate the evolution of the austenite fraction transformed during the two passes, see Fig. 4b. Good agreement is found between the two methods. Higher transformation temperatures are observed for the second pass where the average cooling rate is lower while the austenite conditions are similar, i.e. most of Nb is in solution and the prior austenite grain sizes are the same in the two passes (see Fig. 4a). Thus, LUMet provides a suitable tool to in-situ measure the microstructure evolution during simulated rapid heat treatment cycles for the HAZ in the investigated type of linepipe steels.

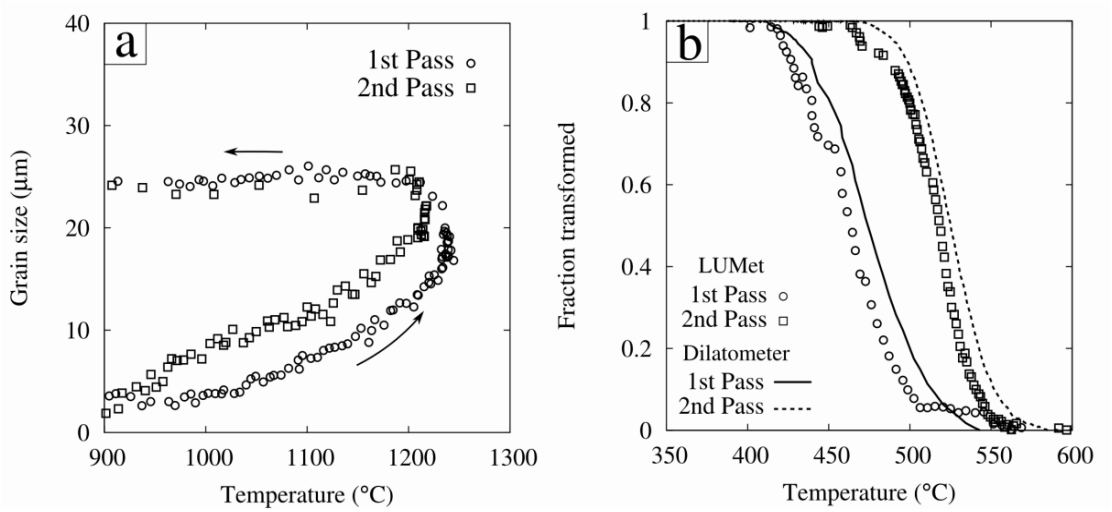

Fig. 4 Microstructure evolution for simulated HAZ dual torch welding cycle in the API-X80 steel: a) austenite grain growth, b) austenite decomposition

3.2 DP600 steel

3.2.1 Isothermal and continuous heating cycles

The applicability of laser ultrasonics for monitoring the microstructure evolution during processing of cold-rolled DP600 steel through intercritical annealing was also studied. Again the ultrasound velocity and attenuation were recorded for this purpose. The first process to take place upon heating to the intercritical temperature is recrystallization of this cold-rolled structure. Thus, in a first test series, it is attempted to use the evolution of ultrasonic velocity during isothermal annealing to monitor recrystallization. An example for these isothermal studies is shown in Fig. 5 for an annealing temperature of 625 ºC. Relatively small changes in velocity are observed in the initial stages of annealing. Subsequently, the ultrasonic velocity significantly increases by approximately 110 m/s to eventually reach a constant value. As described elsewhere [20], recrystallization was also measured using conventional metallographic techniques. Comparing the metallographic recrystallization data with the ultrasonic velocity clearly indicates that the changes in ultrasound velocity correlate with recrystallization. To further confirm this finding, the recrystallized sample is subjected to the same isothermal heat treatment where a constant ultrasound velocity is measured.

In a polycrystalline material, the bulk modulus is affected by texture due to elastic anisotropy. Therefore, in a first approximation, the changes in ultrasound velocity reflect the evolution of texture during recrystallization. The changes in texture, i.e. the strengthening of the gamma-fiber, in the course of recrystallization were measured by Zhu and Militzer [22] for the same cold-rolled steel employed in the present study. Faster recrystallization of grains belonging to the high stored energy gamma-fiber compared to the alpha-fiber is typically observed, see e.g. [23]. The orientation distribution thus remains unchanged, when recrystallization is confined to the gamma-fiber; this explains the relative constancy of ultrasonic velocity during the first 40 pct of recrystallization. Similar observations were made based on the calculations of ultrasonic velocity using experimentally measured texture at different stages of recrystallization for interstitial-free steel [11].

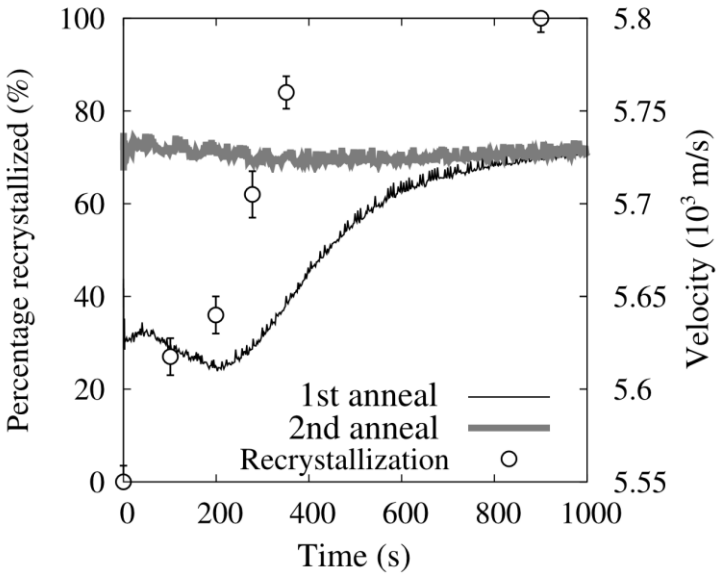

Fig. 5 Evolution of ultrasound velocity and metallographic recrystallization data during isothermal annealing of DP600 steel at 625 ºC

Subsequently, the laser ultrasonic measurements were extended to monitor microstructure evolution during continuous heating where austenite formation takes place in addition to recrystallization. The changes in ultrasonic velocity, as well as conventional measurements of recrystallization and austenite formation during continuous heating at 1 ºC/s are shown in Fig. 6a. During heating up to 670 ºC, the ultrasound velocity decreases nonlinearly due to the nonlinear temperature dependence of magnetic ordering and elastic constants. The ultrasonic velocity starts to increase after 670 ºC where approximately 35 pct of recrystallization is observed metallographically. Following complete recrystallization at 700 ºC, the velocity decreases again upon further heating. Similar to the continuous heating simulations in the API-X80 steel, the austenite formation is not associated with significant changes in velocity due to similar elastic properties of ferrite and austenite at this temperature. The discontinuity at 745 ºC is attributed to the magnetic transition at the Curie temperature, as observed in the API-X80 steel and reported for other low alloy steels [14,24]. The velocity decrease measured between 745 ºC and 830 ºC coincides with the two phase temperature region as measured by dilatometry. The linear temperature dependence for austenite is measured above 830 ºC with a similar slope than that measured for the API-X80 steel. The onset of the linear velocity variation correlates well with completion of austenite formation.

Increasing the heating rate to 10 ºC/s, some important changes were observed in the variation of ultrasound velocity with temperature (see Fig. 6b). At lower temperatures, the velocity decreased monotonically up to 745 ºC without showing the typical region of velocity change due to recrystallization. At this temperature, metallographic observation indicates that only 30 pct of the recrystallization is completed. According to the observation in Fig. 5, this recrystallized fraction may not be large enough to modify the elastic property in the propagation direction. Above the Curie temperature discontinuity at 745 ºC, the velocity stays almost constant up to 785 ºC where it decreases again up to the austenite completion temperature measured by dilatometry. The peculiar velocity change between 745 and 830 ºC is attributed to concurrent recrystallization and austenite formation as shown with metallographic investigations in a previous study [20]. Further analysis is however required at this stage to be able to readily determined from velocity measurements, the completion temperature of recrystallization and/or austenite formation in case where both transformations

occur concurrently. Above 830 ºC, the classical linear decrease of the velocity is measured in good agreement with the behaviour in single phase austenite. Further, unlike in the API-X80 steel, attenuation data for the DP600 steel are inconclusive to record austenite formation.

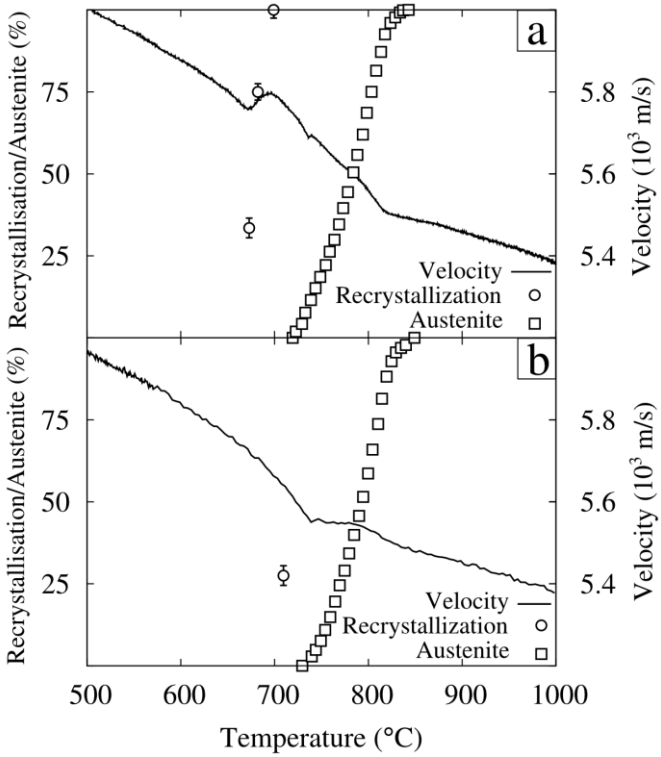

Fig. 6 Recrystallization, austenite formation and changes in laser ultrasonic velocity during continuous heating of the DP600 steel at (a) 1 ºC/s and (b) 10 ºC/s

3.2.2 Simulation of intercritical heat treatment cycle

The capabilities of laser ultrasonics are now well established to monitor recrystallization, austenite formation and decomposition in the cold-rolled DP600 steel. Thus, the microstructure evolution can be monitored during an entire intercritical annealing cycle. The investigated thermal path is given in Fig. 1b. Fig. 7 shows the evolution of the ultrasound velocity and the austenite volume fraction as measured from dilatometry. The increase of velocity measured during recrystallization is already discussed above. The observed local velocity maximum is indicative of completion of recrystallization at 700 ºC. During intercritical annealing at 770 ºC, the ultrasound velocity remains constant while the austenite content increases from 15 to 45 pct. This confirms that ultrasound velocity is insensitive to the formation of austenite in this steel. However, the velocity measured upon cooling from 770 ºC to 465 ºC (i.e. between approximately 1350 and 1450 s in Fig. 7) shows a non-linear temperature dependence that is consistent with the presence of ferrite in the structure. Although dilatometer measurements show a reduction of the austenite content from 45 to 25 pct during this cooling portion, the velocity change does not provide any quantitative measure of austenite decomposition. Indeed, the velocity lever–rule method described above requires the low temperature extrapolation of the velocity in a fully austenitic structure which is not measured in this case. At 465 ºC the sample was held for 180 s to simulate the thermal cycle of a hot dip galvanizing step. The velocity increases by approximately 25 m/s during the isothermal holding at this temperature. This change is associated with the formation of bainite in the microstructure and is consistent with a large difference in the velocity of austenite and bainite at this temperature as demonstrated in Fig 3. In conclusion, this measurement indicates

that LUMet can monitor the isothermal bainite transformation similarly to what is observed during continuous cooling in the API-X80 steel (see Fig. 3 and 4b). The final intercritically annealed DP600 microstructure is shown in Fig. 8 and consists of 70 pct ferrite, 20 pct bainite and 10 pct martensite.

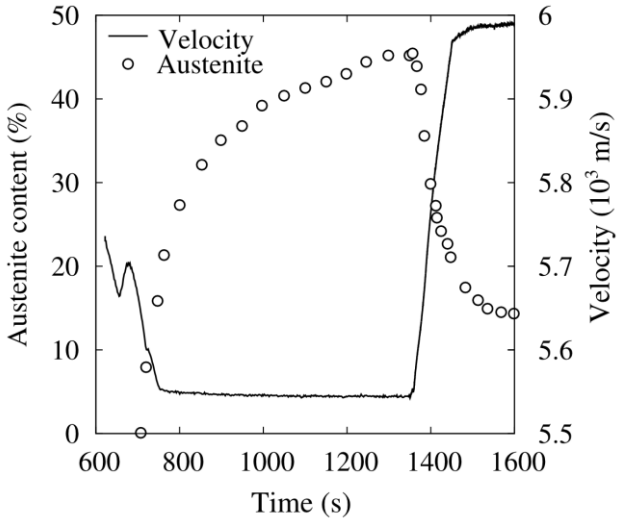

Fig. 7 Microstructure evolution during intercritical annealing cycle of DP600 steel

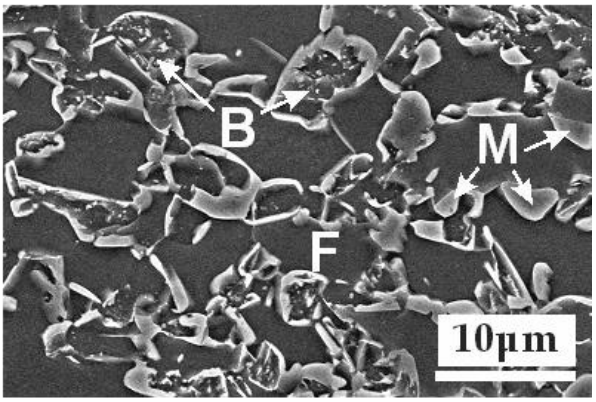

Fig. 8 Final microstructure of DP600 steel after complete intercritical annealing cycle (F: ferrite, B: bainite, M: martensite)

4. Conclusions

In summary, laser ultrasonics is an attractive tool complementing more traditional methods, i.e. metallography and dilatometry, for monitoring microstructure evolution during heat treating cycles of advanced steels. Two important heat treatment cycles were simulated: (i) rapid thermal cycles of the HAZ during welding of an API-X80 linepipe steel, (ii) intercritical annealing cycles for a DP600 steel. Laser ultrasonics is an excellent tool to monitor austenite grain growth in the HAZ thermal cycles since attenuation provides a reliable measure of grain size. Phase transformations and recrystallization, on the other hand, modify the crystal structure and/or texture of the material probed and can, thus, be monitored with ultrasound velocity. The present investigation shows that austenite-ferrite transformations can be accurately measured by laser ultrasonics provided the transformation temperatures are below the Curie temperature where ultrasound velocities are sufficiently different in austenite and ferrite. At higher temperatures, however, ultrasound velocity does not provide any quantitative

data on this phase transformation and thereby limiting its applicability to monitor intercritical austenite formation. Additional studies are required to further explore the potential to use attenuation to record the austenite-ferrite transformations above the Curie temperature. Large variations of attenuation during austenite formation have been repeatedly obtained for the linepipe steel but not for the DP steel. On the hand, recrystallization in the DP steel during heating of cold-rolled sheets can be monitored with laser ultrasonics but this is limited to recrystallization stages where strong texture changes occur (e.g. between 35 and 100 pct recrystallized in the investigated DP600 steel). Further, laser ultrasonics can provide some information on whether or not recrystallization is completed before austenite formation. The absence of the characteristic velocity maximum for completion of recrystallization may be taken as an indication of concurrent recrystallization and austenite formation.

These examples show the significance of this new sensor technology for in-situ microstructure measurements during thermomechanical processing of steel. A main advantage of LUMet is that it is a fast and remote technique that probes the bulk of the material. Thus, the use of the LUMet system enables to study microstructure evolution much more rapidly for many different processing paths than would be possible with conventional techniques. As a result, LUMet can significantly accelerate the development and validation of metallurgical process models for advanced steels. While there are limitations, the LUMet system offers exciting opportunities for alloy and process development in the laboratory. Further evaluations are required to assess LUMet as a microstructure process control system in the plant.

Acknowledgement
The authors acknowledge the financial support received from the Natural Sciences and Engineering Research Council of Canada (NSERC), Evraz Inc. NA (Regina, SK), TransCanada Pipelines Ltd. (Calgary, AB) and ArcelorMittal Dofasco Inc. (Hamilton, ON, Canada).

References

[1] Zhao M, Yang K and Shan Y. The effects of thermo-mechanical control process on microstructures and mechanical properties of a commercial pipeline steel[J]. Mater Sci Eng A, 2002, 335(1-2): 14-20.
[2] Zhao W, Wang W, Chen S and Qu J. Effect of simulated welding thermal cycle on microstructure and mechanical properties of X90 pipeline steel[J]. Mater Sci Eng A, 2011, 528(24): 7417-7422.
[3] Lambert-Perlade A, Gourgues A F and Pineau A. Austenite to bainite phase transformation in the heat-affected zone of a high strength low alloy steel[J]. Acta Mater, 2004, 52(8): 2337-2348.
[4] Banerjee K, Militzer M, Perez M and Wang X. Nonisothermal austenite grain growth kinetics in a microalloyed X80 linepipe steel[J]. Metall Mater Trans A, 2010, 41(12): 3161-3172.
[5] Poole W J, Militzer M and Garcin T. Integrated model to predict microstructure and mechanical properties in the heat affected zone for X80 linepipe[C]. International Pipeline Conference. Calgary, AB, Canada, September 2012: 90337.
[6] Senuma T. Physical metallurgy of modern high strength steel sheets[J]. ISIJ Int, 2001, 41(6): 520-532.
[7] Monchalin J P. Laser-Ultrasonics: From the laboratory to industry[C]. AIP Conf. Proc., Quantitative Nondestructive Evaluation. Green Bay, WI, August 2003: 700, 3-31.
[8] Dubois M, Militzer M, Moreau A and Bussière J F. A new technique for the quantitative

real-time monitoring of austenite grain growth in steel[J]. Scr Mater, 2000, 42(9): 867-874.

[9] Kruger S E, Lamouche G and Monchalin J P. On line monitoring of wall thickness and austenite grain size on a seamless tubing production line at the Timken Company[J]. Iron Steel Tech 2005, 2: 25-31.

[10] Maalekian M, Radis R, Militzer M, Moreau A and Poole W J. In situ measurement and modelling of austenite grain growth in a Ti/Nb microalloyed steel[J]. Acta Mater, 2012, 60(3): 1015–1026.

[11] Hutchinson B, Lindh-Ulmgren E and Carlson L. Application of laser ultrasonics to studies of recrystallisation and grain growth in metals[C]. 1st Internat. Symposium on Laser Ultrasonics, Science, Technology and Applications. Montreal, PQ, Canada, July 2008, 31: 1-6.

[12] Kruger S E, Lamouche G, Moreau A and Militzer M. Laser ultrasonic monitoring of recrystallization of steels[C]. MS&T Materials Science and Technology Conference Proceedings, John Wiley and Sons Ltd. New Orleans, LA, US, September 2004, 21: 809-813.

[13] Sarkar S, Moreau A, Militzer M and Poole W J. Evolution of austenite recrystallization and grain growth using laser ultrasonics[J]. Metall Mater Trans A, 2008, 39(4): 897-907.

[14] Smith A, Kruger S E, Sietsma J and Van der Zwaag S. Laser-ultrasonic monitoring of austenite recrystallization in C–Mn steel[J]. ISIJ Int. 2006, 46(8): 1223-1232.

[15] Dubois M, Moreau A, Militzer M and Bussière J F. Laser-ultrasonic monitoring of phase transformations in steels[J]. Scr Mater, 1998, 39(6): 735-741.

[16] Dubois M, Moreau A and Bussiere J F. Ultrasonic velocity measurements during phase transformations in steels using laser ultrasonics[J]. J Appl Phys, 2001, 89(11): 6487-6495.

[17] Ing R K, Monchalin J P. Broadband optical detection of ultrasound by two-wave mixing in a photorefractive crystal[J], Appl Phys Letters, 1991, 59(1): 3233-3235.

[18] Militzer M, Maalekian M, Garcin T and W J Poole. Microstructure evolution model for the HAZ of girth welds in X80 linepipe steel[C]. Welding of High Strength Pipeline Steels. TMS, Warrendale, PA, US, 2011: in press.

[19] Dever D. Temperature dependence of the elastic constants in alpha-iron single crystals: relationship to spin order and diffusion anomalies[J]. J Appl Phys, 1972, 43: 3293-3301.

[20] Kulakov M, Poole W J and Militzer M. The Effect of the initial microstructure on recrystallization and austenite formation in a DP600 steel[J]. Metall Mater Trans A, 2013: in press.

[21] Coronel V F, Beshers D N. Magnetomechanical damping in iron[J]. J Appl Phys, 1988, 64(4): 2006-2015.

[22] Zhu B and M. Militzer. 3D phase field modelling of recrystallization in a low-carbon steel[J]. Modell. Simul. Mater Sci Eng, 2012, 20: 085011.

[23] Oyarzabal M, de Guerenu A M and Gutierrez I. Effect of stored energy and recovery on the overall recrystallization kinetics of a cold rolled low carbon steel[J]. Mater Sci Eng A, 2008, 485: 200-209.

[24] Kruger S and Damm E. Monitoring austenite decomposition by ultrasonic velocity[J]. Mater Sci Eng A, 2006, 425: 238-243.